DØnote 4490-CONF

A Search for RPV–SUSY in the $\mu\mu\ell$ (ℓ=e,μ) Channel from Decays via the LL$\overline{\text{E}}$–coupling λ_{122}

Daniela Käfer, Arnd Meyer

(Dated: July 24, 2004)

This note describes the search for two different trilepton signatures ($\mu\mu\mu$ and $\mu\mu$e) from R-parity conserved (RPC) production of supersymmetric particles followed by an R-parity violating (RPV) decay via the coupling λ_{122}. Data collected from April 2002 to September 2003 with the DØ-detector at the Fermilab Tevatron with a center of mass energy of 1.96 TeV are analyzed. The data correspond to an integrated luminosity of $\mathcal{L}$ =160.3±10.4 pb^{-1}.

In the selected $\mu\mu\mu$-sample 0.56±1.40 events are expected within the Standard Model (SM) while one event is observed in data. One event is also seen in the $\mu\mu$e channel with an expectation of 0.07±1.33 events from SM-processes. The corresponding cross section limits, of the order of 0.2 to 0.3 pb, are interpreted in the framework of the mSUGRA model for different sets of parameters m_0, $m_{1/2}$, tan(β)=5, A_0=0 and both signs of the higgsino mass parameter μ. For μ <0 neutralino masses up to 84 GeV and chargino masses ($\tilde{\chi}_1^{\pm}$) up to 160 GeV can be excluded and for μ >0 the exclusion limits lie about 6 GeV higher.

Preliminary Results for Summer 2004 Conferences

I. INTRODUCTION

Multilepton final states are expected in most SUSY-models if the lightest SUSY-particle is allowed to decay into a purely leptonic state, i.e. via one of the LL$\overline{\text{E}}$-couplings λ_{ijk}. In this analysis the RPV-coupling λ_{122} is investigated, while all other RPV-couplings are considered to be negligibly small. It is assumed that the SUSY-particles are RPC-produced, which means that SUSY-particles are produced pairwise, see also [1].

Once produced, the sparticles (mostly neutralinos and charginos) decay predominantely into pairs of the lightest neutralinos ($\tilde{\chi}_1^0$), which in turn can only decay further into SM-particles by violating R-parity. These two assumptions lead to final states with at least four charged leptons in processes where one of the LL$\overline{\text{E}}$-couplings is involved. Figure 1 shows the four possible decay modes: $\mu^+\mu^-\nu_e$, $\mu^-\mu^+\bar{e}_\mu$, $e^-\mu^+\bar{\nu}_\mu$ and $e^+\mu^-\nu_\mu$ which can be combined into three different multilepton final states or signatures: $\mu\mu\mu\mu$, $\mu\mu\mu e$, and $\mu\mu ee$.

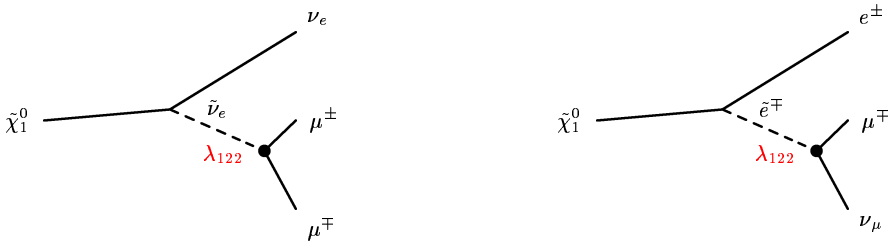

FIG. 1: The Feynman graphs for the RPV-decays of $\tilde{\chi}_1^0$ via the coupling λ_{122}.

There are at least four charged leptons expected in these final states. As the $\tilde{\chi}_1^0$-mass is expected to be relatively small, ($M_{\tilde{\chi}_1^0} \approx$ 50-90 GeV), the leptons are low p_T objects and thus difficult to detect. Therefore only three charged leptons are required to be present and the analysis is optimized with respect to the following two channels: $\mu\mu\mu$ and $\mu\mu$e. The rate for all possible combinations of three charged leptons is $3:4:1$ for $\mu\mu\mu:\mu\mu e:\mu$ee, respectively. The decay channel μee is covered in a separate analysis [2].

II. THE DATA SAMPLE

Data collected with the DØ-detector [3] between April 2002 and September 2003, corresponding to an integrated luminosity of $\mathcal{L}$ =160.3$\pm$10.4 pb^{-1} are analyzed. Only data with fully functional Muon system, Central Fiber Tracker (CFT), Silicon Microstrip Tracker (SMT), and calorimeter are considered. Events are required to be triggered by dimuon triggers based on the muon system, for part of the data in coincidence with a track candidate in the CFT.

III. MONTE CARLO SAMPLES

The analyzed Monte Carlo samples are split into the SM-processes that are the "known" backgrounds for this analysis and the signal processes which have been generated with SUSYGEN [4]. This MC-generator uses the separate program SUSPECT [5] for the evolution of the Renormalization Group Equations.

Standard Model background processes are simulated with PYTHIA (versions: 6.201 and 6.202, see also [6]). All considered SM-processes, as well as the cross section $\sigma_{MC} \times$ BR, the equivalent luminosity, and the number of generated events can be found in the appendix in table IV.
For the generation of the signal samples CTEQ5L PDFs [8] are used and all samples are processed through the full detector simulation. The events are combined with an average of 0.8 minimum bias events and are reconstructed using the same program as the data. Table V in the appendix provides an overview of all analyzed SUSY-points with the two dominant production processes chargino+chargino (CC) and neutralino+chargino (NC) shown separately. The value of the coupling is chosen to be λ_{122} =0.001 but this value mostly influences the lifetime of the $\tilde{\chi}_1^0$, which is below 0.1 mm for all points that are analyzed here. Neither the event topology nor the mass spectrum or the decay branching fractions depend on the size of the λ_{122} coupling.

IV. OBJECT IDENTIFICATION AND EFFICIENCIES

All objects (muons, electrons, jets, missing transverse energy) are identified and selected according tothe standard DØ object identification criteria. Jets and missing transverse energy objects (MET) are corrected based on the current knowledge of the detector resolution and energy scale.

A. Muon candidates

Each muon candidate in an event is required to be of "loose" quality and have a transverse momentum of at least 2 GeV. Timing cuts based on scintillator information are applied to reject cosmic muons. Additionally, the two leading muons must also meet the following requirements:

- at least 8 hits in the CFT-detector
- hits in all layers or at least in the "post-toroid" (BC) layer, and a matched central track

The reconstruction efficiencies for data and MC ε_{reco} are determined with muons that have been identified in the calorimeter. Events where one muon is required to be loose, matched to a central track and with a p_T >20 GeV and the other muon (measured in the calorimeter) should have a p_T >10 GeV, are selected. Moreover the two muons are required to be separated by $\Delta\phi$ >2.5. Then the calorimeter muon is tested wether it is of at least loose quality or not. For the determination of the trackmatching efficiencies ε_{trkm} events with two loose muons with a transverse momentum p_T >15 GeV, separated by $\Delta\phi$ >2.5 and where both muons are isolated are selected. Then the product of tracking and track matching efficiency is measured.
The isolation efficiencies are also determined separately for data and MC with events from Z-decays: Again two loose muons with p_T >15 GeV, a separation of $\Delta\phi$ >2.5 and this time both muons matched to a central track are required per event. Additionally the invariant mass calculated from these muons must be in a window of ± 20 GeV around the Z-mass. One muon must also satisfy the isolation requirements while the other muon is tested for isolation.

B. EM candidates

Each electromagnetic (EM) candidate in an event should satisfy the following criteria:

- a cluster in the calorimeter compatible with an electromagnetic object
- $emf > 0.9$, where emf denotes the fraction of EM-energy versus total energy deposit
- $iso = \frac{E_{tot}(R<0.4) - E_{em}(R<0.2)}{E_{em}(R<0.2)} < 0.15$, where E_{tot} (E_{em}) denotes the total energy (EM-energy) deposited in a cone with the specified radius R =0.4 (0.2), with $R = \sqrt{(\Delta\phi)^2 + (\Delta\eta)^2}$

The efficiencies for the identification of EM-candidates and the electron likelihood are determined in the following way: Events which have one good electron that satisfies the above criteria are selected. Additionally one isolated track is required and the invariant mass calculated from this track and the electron must lie in a mass window of ± 40 GeV around the Z mass. This track is then tested for a matching electromagnetic cluster in a window of 0.1×0.1 in $\eta \times \phi$ around the track. The energy deposition in the calorimeter must satisfy the electron identification criteria. The same method is used to determine this efficiency in a $Z/\gamma^* \rightarrow ee$ MC. Remaining differences between data and simulation are corrected by applying correction factors to Monte Carlo events.
For the determination of the efficiency of a cut on the electron likelihood two good EM clusters are selected, again within a mass window of ± 40 GeV around the Z-mass. Then it is tested how many of these EM clusters pass the cut of 0.3 on the electron likelihood, and again correction factors are derived.

C. Missing transverse energy (MET)

MET-objects are corrected for the JetEnergyScale (JES), and corrections for electromagnetic particles (since the response of the calorimter is different for hadrons and EM-particles) and also for muons are applied.

D. Jet-ID

All jets are calorimeter objects defined by the following criteria:

- $0.05 <$ EMF < 0.95 (EMF: electromagnetic fraction)
- CHF < 0.4 (CHF: fraction of the jet energy deposited in the "coarse hadronic" section of the calorimeter)
- HotF < 10 (HotF: "hot" fraction, ratio of highest to second highest cell-E_T)
- n90 > 1 (number of towers which contain at least 90% of the energy)
- $L1set \;/\; p_{T,jet} \cdot (1 - CHF) > 0.4$ (in central (CC) and endcap (EC) calorimeters), > 0.2 (in ICD)

where L1set is the scalar transverse energy of all L1 trigger towers in a cone of radius ΔR <0.5. This energy from the first trigger level is then compared to the jet E_T read out from the calorimeter (minus the coarse hadronic fraction). Here CC is defined as the detector region with $|\eta_{det}|$ <0.8, EC as $|\eta_{det}|$ >1.5 and ICD is the inter cryostat region with $0.8 < |\eta_{det}| < 1.5$. The calorimeter cells are clustered with a cone algorithm (cone radius: ΔR=0.5) and subsequently a JetEnergyScale correction is applied. All jets are required to have a minimum E_T of 8 GeV.

V. TRIGGER EFFICIENCIES FOR DATA AND MC

The trigger efficiency for every MC-sample is obtained using independent data samples. The probability of an event to fire the trigger is applied as a weight to all MC events (SM backgrounds and signal) in the same way. The weighting takes into account the p_T, η and ϕ information of all physical objects in the event, i.e. muons, EM-objects, jets and the missing transverse energy (MET). The parameterizations of the efficiencies for all triggers are split into the corresponding trigger levels (L1, L2 and L3). These parameterizations are based on offline measurements of the efficiencies for the different objects.

VI. ESTIMATION OF QCD BACKGROUND CONTRIBUTION FROM DATA

Semileptonic events from multi-jet processes (mostly $b\bar{b}$ and $c\bar{c}$) are expected to dominate this kind of background. In order to not use the phase space region where the signal is expected to lie, a like-sign (LS) sample with special isolation requirements is chosen to estimate the QCD contributions to the SM background expectation. This sample will contain essentially events from semileptonic b- and c-decays, which is the dominating QCD part in the unlike-sign (ULS) sample as well. The main differences between the two samples (LS and ULS) are the decay chains and the production rates. Most of the b- and c-decays arise from direct production via gluon-gluon fusion and flavor excitation, resonances like J/Ψ or Υ are small compared to the inclusive production.

Events with two like-sign muons of loose quality are selected from the analysis sample. Like-sign muons are chosen because the QCD-background will dominate in this sample since for most other SM processes (like Z/γ^*, WW or Υ production) events with two unlike-sign leptons are expected. This sample is then split again into two subsamples: events where both muons satisfy the tight isolation criteria (refered to as "iso"-sample) and a second subsample containing events where one of the two muons is tightly isolated, and the other muon is "almost" isolated. The "almost" isolated muon is defined by softened isolation criteria in order to obtain a kinematically similar sample to the isolated selection. If a muon already satisfies one of the soft isolation criteria (either the calorimeter or the track-isolation) then the other muon may meet the soft or the tight criterion. Another reason for the choice of an "almost" isolated sample is the fact that in the subsequently described DiMuon-selection the two leading muons are required to be tightly isolated, except for the QCD estimation itself. The ratio $R = {}^{\text{iso}}/_{\text{almost}}$ is calculated from the number of isolated DiMuon-pairs versus the transverse momentum of the most energetic muon and the number of almost isolated DiMuon-pairs versus the p_T of the almost isolated muon. This ratio R is then used to weight the p_T-spectrum of the "almost"-sample sinde a correlation between the isolation requirements and the p_T-spectra is expected. This can be explained in the following way: lower p_T muons are more likely to get "kicked away" from the b-jet and are thus more isolated than higher p_T muons for which the kicking is not as effective.

In a last step the reweighted QCD sample is scaled to the data after subtracting all other expected backgrounds. To achieve agreement between the remaining data and the estimated QCD background an overall scaling factor of 2.7 is applied. The uncertainty on the QCD background estimate is – after all cuts – dominated by its statistics. The systematic uncertainty is estimated to be 50%, based on the uncertainty in the reweighting factor: assuming that the p_T-spectrum of the "almost"-sample would not need any reweighting.

VII. THE DIMUON SELECTION

After optimization studies with respect to the purity×efficiency of the signal ($p \cdot \varepsilon_{sig} = \varepsilon_{sig} \cdot S/\sqrt{S+B}$) at the end of the DiMuon selection, the following cuts are applied sequentially. The cuts are optimized for one SUSY point, namely $\mathcal{P}2neg$. Muons are considered within the full coverage of the DØ muon system (η=2.1).

- cut 1: $p_T(\mu 1) > 11$ GeV, $p_T(\mu 2) > 6$ GeV as measured in the central tracking detectors
- cut 2: both muons are required to be tightly isolated (except QCD background sample)
- cut 3: $\Delta R(\mu 1, \mu 2) > 0.2$ and $\Delta R(\mu 1/2, jet) > 0.5$
- cut 4: $|z_{vertex}| < 60$ cm of the nominal interaction point and $|z(\mu 1) - z(\mu 2)| < 0.5$ cm
- cut 5: $M_{\mu 1 \mu 2} < 6$ GeV$/(-6.5 \cdot 10^{-4} \cdot \mathrm{MET} + 0.027$ GeV$) + 240$ GeV and
  $M_{\mu 1 \mu 2} > -4.4 \cdot \mathrm{MET} + 75$ GeV
- cut 6: MET$> -4 \cdot (p_T(\mu 1) + p_T(\mu 2)) + 80$ GeV and
  MET$> 0.5 \cdot (p_T(\mu 1) + p_T(\mu 2)) - 20$ GeV
- cut 7: $\Delta\phi(\mu 1 \mu 2) < 2.6$ for $80 < M(\mu^+\mu^-) < 100$ GeV

The two-dimensional cuts 5 and 6 are chosen in order to improve the signal efficiency compared to a simple one-dimensional selection. As an example, figure 2 illustrates cut 5, where one cut in the M_{inv}-MET plane is intended to reduce the background of low p_T Z/γ^*, Υ production,and QCD, whereas the second cut is intended to lower the background from high p_T Z/γ^* processes. Similar arguments hold for cut 6 in the DiMuon-selection. Cut 7 is chosen because of the back-to-back nature of Z/γ^* decay products in the (r, ϕ)-plane.
Table I gives an overview of event numbers for all SM background processes and the data after all sequential DiMuon selection cuts. After all cuts, a good agreement between data and Monte Carlo expectation is seen 3.

TABLE I: The cut flow of the DiMuon selection is shown for all SM background processes, the sum of all MC-samples in comparison with data and the signal efficiency for the SUSY point $\mathcal{P}4neg$ (see appendix). Included are statistical errors and systematic uncertainties due to the luminosity measurement, the trigger efficiency and all MC correction factors.

	$Z/\gamma^* \to \mu\mu/\tau\tau$	QCD/Υ(1s,2s)	WW, WZ, $t\bar{t}$	Backgr.-sum	Data	SUSY-P4neg
Dimu	$N \pm stat \pm sys$	$N \pm stat \pm sys$	$N \pm stat \pm sys$	$N \pm stat \pm sys$	N	$N \pm stat \pm sys$
cut 1	10638.4±35.7±645.4	673.4±12.4±217.5	8.30±0.31±0.68	11320.1±37.8±681.1	10950	47.47±0.65±2.72
cut 2	7894.9±28.6±509.0	290.4±9.9±86.3	5.97±0.31±0.50	8191.3±30.3±516.3	8073	21.57±0.53±1.23
cut 3	7569.7±28.6±485.3	269.5±8.8±82.3	5.58±0.30±0.47	7844.8±30.0±492.2	7790	20.80±0.52±1.19
cut 4	7555.6±28.1±485.3	256.5±8.2±80.5	5.58±0.30±0.47	7817.9±29.3±491.9	7743	20.78±0.52±1.19
cut 5	449.4±7.0±21.7	26.4±4.2±9.6	4.20±0.30±0.39	480.0±8.2±23.7	502	18.40±0.50±1.05
cut 6	366.9±6.5±16.9	26.4±4.2±9.6	4.03±0.30±0.39	397.3±7.7±19.4	411	17.52±0.49±1.00
cut 7	273.3±5.9±13.0	26.4±4.2±9.6	3.56±0.30±0.36	303.3±7.3±16.1	343	16.93±0.48±0.97

VIII. THE SELECTION OF $\mu\mu\mu$ AND $\mu\mu$e FINAL STATES

The separate search for either $\mu\mu\mu$ or $\mu\mu e$ final states are reflected in the selection cuts. They are chosen such that the quality of the third selected object is ensured. Only very few SM background processes still contribute at this stage of the analysis and most of them, like $t\bar{t}$ production or $WZ \to \mu\nu_\mu\mu\mu\,/\,e\nu_e\mu\mu$ have very small cross sections. The only other relevant contribution comes from QCD multi-jet processes and instrumental (or fake) backgrounds from either noise in the different subdetectors or mismeasured objects. The following cuts are applied:

- $\mu\mu\mu$-cut 1: 3^{rd} μ with $p_T > 3$ GeV
- $\mu\mu\mu$-cut 2: $\Delta R(\mu 1/2, \mu 3) > 0.1$, a matched track and $\Delta R(\mu 3, jet) > 0.2$
- $\mu\mu\mu$-cut 3: all muons from the same vertex: $z(\mu 1/2) - z(\mu 3) < 0.5$ cm

The p_T threshold for the third muon is reduced as much as possible to allow for as many low p_T muons to be selected

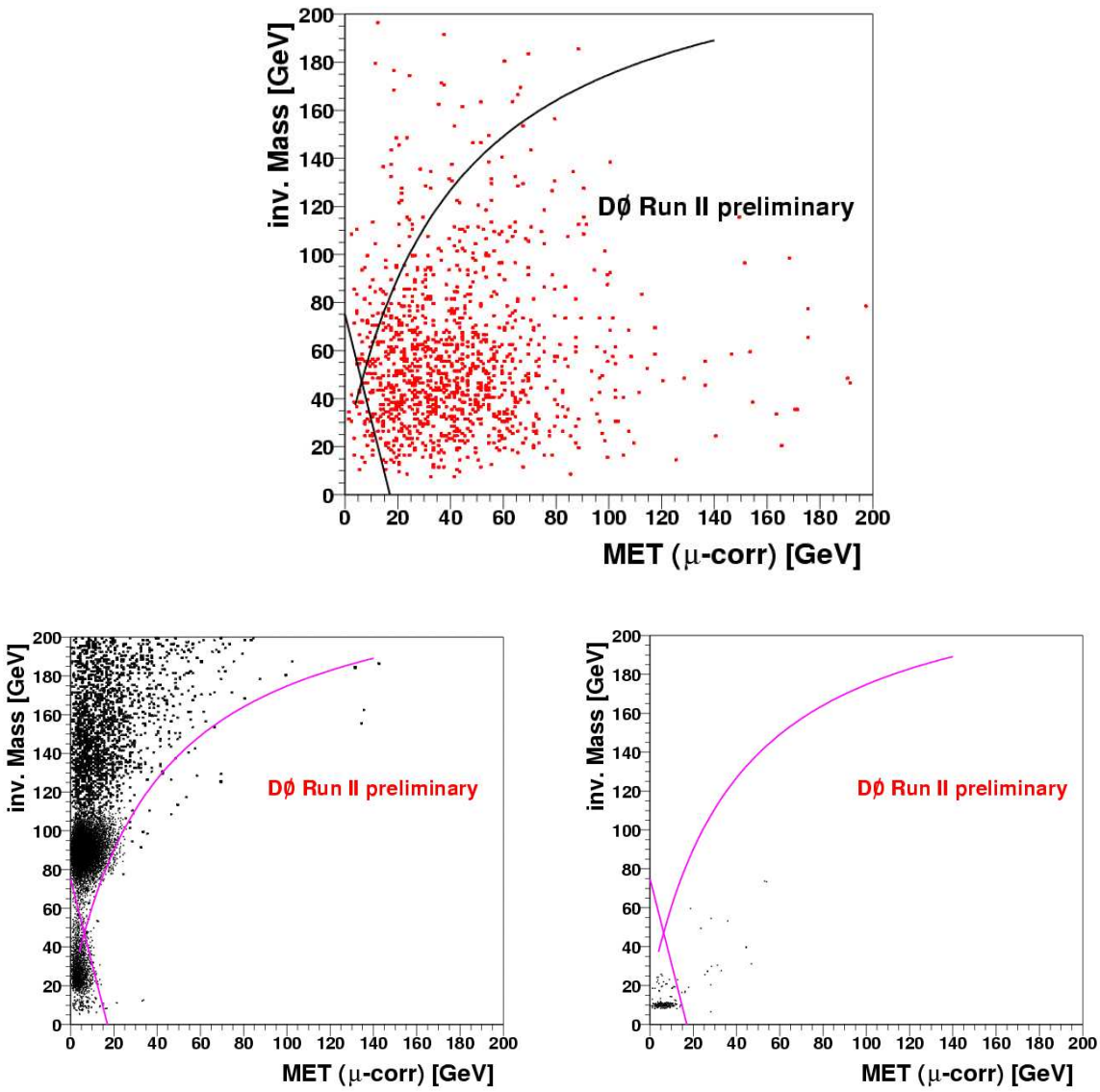

FIG. 2: Illustration of cut 5 in the DiMuon-selection. The signal (point $\mathcal{P}4neg$) is shown in red (upper plot) and the backgrounds in black. Lower left: Z/γ^* and lower right: QCD / Υ-backgrounds.

while still requiring that a muon hits at least the first layer of the muon chambers (A-layer). Muons which are below 1.6 GeV p_T do not reach the muon system at all, but are absorbed in the calorimeter.

- $\mu\mu$e-cut 1: one EM-candidate with $p_T > 5$ GeV and a matched track
- $\mu\mu$e-cut 2: $\Delta R(\mu 1/2, e) > 0.05$
- $\mu\mu$e-cut 3: electron likelihood > 0.3

For the $\mu\mu$e final state it is necessary to not only require a higher p_T threshold to obtain reasonably pure electrons, but also a certain distance to the two leading muons even if the third object is an EM and not a muon candidate. This quality condition ensures that the same object is not selected twice, once as a muon and another time as the EM candidate. Finally, a "loose" cut on the electron likelihood rejects "fake" electrons from QCD background. The corresponding event numbers (data, SM background expectation, and signal efficiencies) can be found in table II.

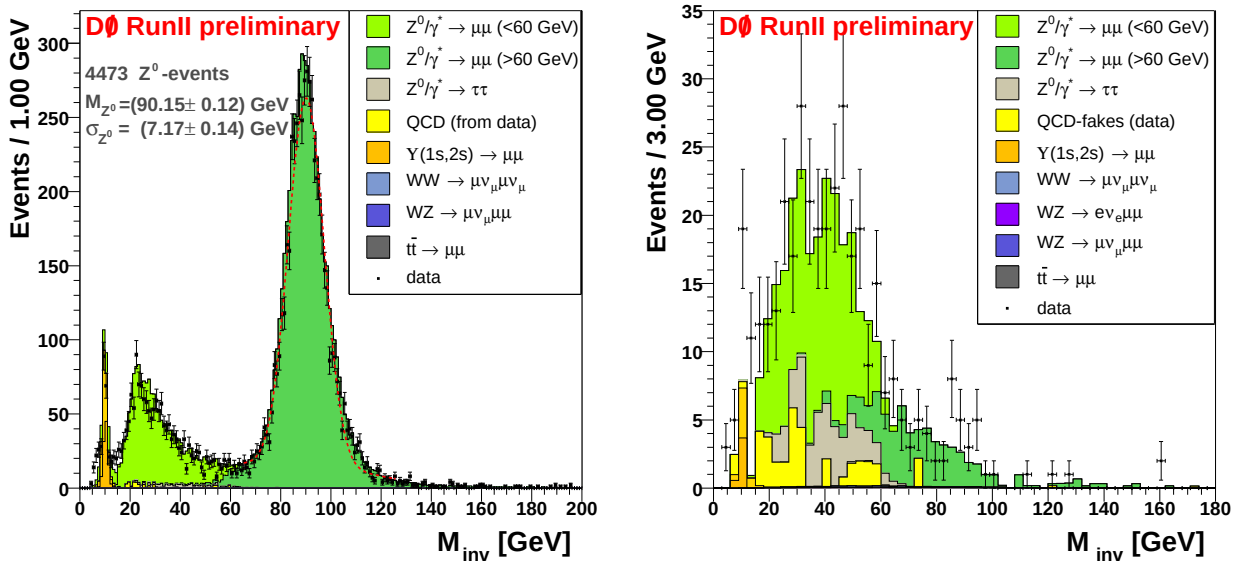

FIG. 3: The DiMuon invariant mass distribution after cut 4 in the selection (left). Both leading muons are isolated and have a matched central track. The dashed red line corresponds to a gaussian + exponential fit to the data. The number of Z candidates in the peak, the fitted Z mass and width are also shown. On the right the distribution of the invariant mass of the two leading muons after the last DiMuon selection cut is shown.

TABLE II: Listed are the background expectations for all SM background MC, the sum of all MC+QCD-estimate in comparison with data. Statistical errors and systematic uncertainties are included as mentioned in the text. The signal efficiency for the SUSY point $\mathcal{P}4neg$ is also presented.

	$Z/\gamma^* \to \mu\mu/\tau\tau$	QCD/$\Upsilon(1s,2s)$	WW, WZ, $t\bar{t}$	Backgr.-sum	Data	SUSY-P4neg
$\mu\mu\mu$	$N \pm stat \pm sys$	$N \pm stat \pm sys$	$N \pm stat \pm sys$	$N \pm stat \pm sys$	N	$N \pm stat \pm sys$
cut 1	1.01±0.36±0.61	<0.63	0.277±0.013±0.037	1.29±1.42	2	8.04±0.36±0.47
cut 2	0.43±0.28±0.61	<0.63	0.126±0.010±0.030	0.56±1.40	1	7.67±0.34±0.44
cut 3	0.43±0.28±0.61	<0.63	0.125±0.010±0.030	0.56±1.40	1	7.62±0.34±0.44
$\mu\mu$e						
cut 1	0.87 ±0.33±0.61	<0.63	0.088±0.010±0.030	0.96±1.40	2	8.85±0.35±0.41
cut 2	<0.67	<0.63	0.080±0.000±0.030	0.08±1.33	1	8.85±0.35±0.41
cut 3	<0.67	<0.63	0.074±0.000±0.030	0.07±1.33	1	6.85±0.33±0.40

IX. SYSTEMATIC UNCERTAINTIES

All systematic uncertainties described in the text have been included in the limit calculation, see also tables I and II. The largest one is, as described, the uncertainty in the QCD background estimate, followed by the 6.5% luminosity uncertainty. Smaller effects taken into account include:

- the uncertainties on the trigger efficiencies for the different Monte Carlo samples
- the uncertainties due to the correction factors (data $\leftrightarrow$ MC)
- the differences between NLO and NNLO K-factors used for the Z/γ^* processes.

All uncertainties are added in quadrature and are also taken into account for the calculation of the limits that are listed in table III. So far no errors due to theoretical uncertainties of the cross sections of SM background processes are considered.

X. RESULTS AND CONCLUSIONS

Data corresponding to an integrated luminosity of $\mathcal{L}$ =160.3±10.4 pb^{-1} has been analyzed with respect to two RPV-SUSY trilepton channels ($\mu\mu\mu$ and $\mu\mu$e). No excess is observed and after all selection cuts, 2 events are seen in data while 0.63±1.93(stat.+sys.) events are expected from SM processes. Thus upper limits are set on the production cross sections for these RPV-SUSY trilepton final states. The limits are calculated based on a Bayesian approach and using the Poisson statistic [10]. In table III the obtained upper limits ($\sigma_{95\%CL}$) together with the corresponding SUSY cross sections (σ_{SUSY}) and the selection efficiencies are listed.
For both signs of the higgsino mass parameter μ the limits are better than the DØ RunI limit, which lies at $m_{1/2}$ ≈160 GeV for m_0=250 GeV[11]. For easier comparison with other RPV SUSY analyses, the 95% CL upper limits are presented versus the neutralino and the chargino mass (figures 4 and 5). For the lightest neutralino ($M_{\tilde{\chi}_1^0}$) the limit is found to be 84 GeV in case of a negative higgsino mass paramter μ and 90 GeVfor positive μ and the limit on the mass of the lightest chargino ($M_{\tilde{\chi}_1^\pm}$) is determined to be 160 GeV for negative μ and 165 GeV for positive μ, respectively. A comparison of the actual limits in the ($m_0, m_{1/2}$)-plane with the old DØ Run I limits can be found in the appendix.

TABLE III: Overview of all 95% CL upper limits, along with the corresponding signal efficiencies and the SUSY cross sections.

SUSY-point		$\mu < 0$	σ's in pb		$\mu > 0$	σ's in pb	
m_0	$m_{1/2}$	ε_{sig} [%]	$\sigma_{95\%CL}$	σ_{SUSY}	ε_{sig} [%]	$\sigma_{95\%CL}$	σ_{SUSY}
250	140	11.18±0.43±0.60	0.308	1.411	–	–	–
250	150	11.40±0.44±0.63	0.303	1.028	14.69±0.39±0.95	0.236	2.921
250	160	12.02±0.45±0.70	0.288	0.764	15.91±0.52±0.97	0.217	1.962
250	170	–	–	–	16.96±0.53±1.03	0.205	1.239
250	180	14.47±0.48±0.86	0.239	0.437	16.49±0.51±1.01	0.209	0.887
250	200	14.46±0.49±0.84	0.239	0.257	17.23±0.54±1.02	0.201	0.477
250	220	15.67±0.42±0.91	0.219	0.155	17.80±0.52±1.05	0.193	0.269
250	240	–	–	–	18.34±0.44±1.10	0.188	0.157
250	260	–	–	–	19.54±0.74±1.21	0.178	0.098

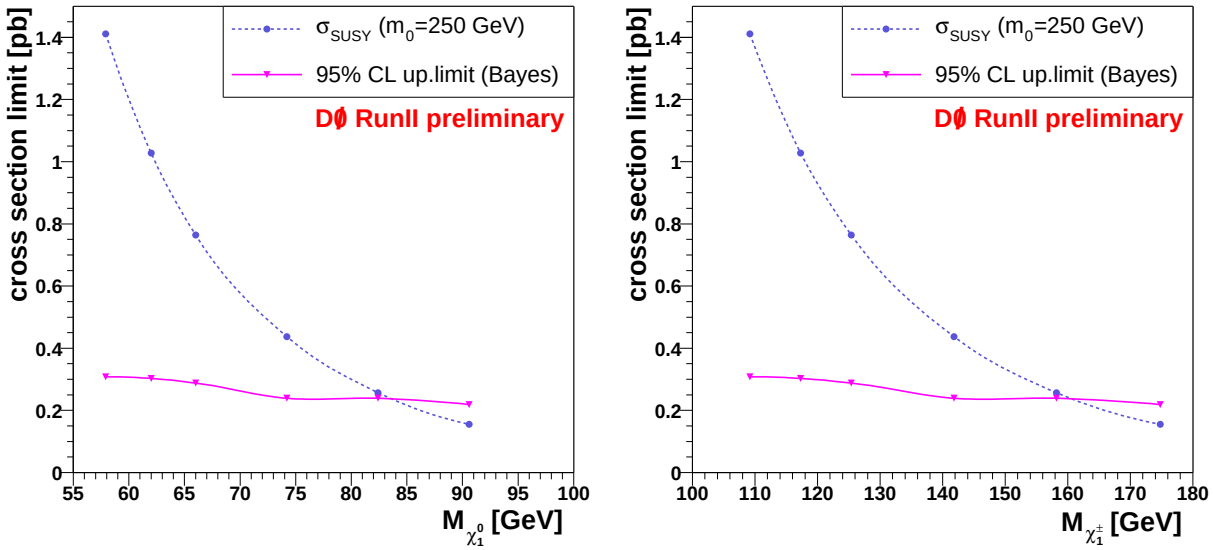

FIG. 4: The 95% CL upper limits on the SUSY cross section (σ_{SUSY}) for fixed m_0 =250 GeV, tan(β)=5, A_0=0 and negative higgsino mass parameter are shown versus $M_{\tilde{\chi}_1^0}$ (left) and versus $M_{\chi_1^\pm}$ (right).

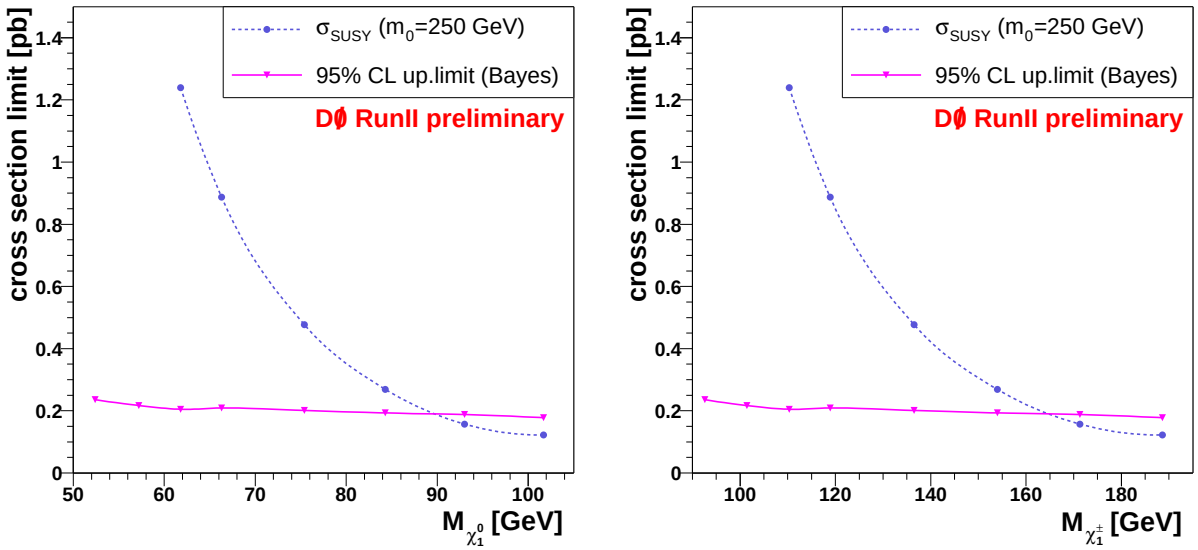

FIG. 5: Illustration of the 95% CL upper limits on the SUSY cross section (σ_{SUSY}) for fixed m_0 =250 GeV, tan(β)=5, A_0=0 and positive higgsino mass parameter versus $M_{\tilde{\chi}_1^0}$ (left) and versus $M_{\chi_1^\pm}$ (right).

Acknowledgments

We thank the staffs at Fermilab and collaborating institutions, and acknowledge support from the Department of Energy and National Science Foundation (USA), Commissariat à l'Energie Atomique and CNRS/Institut National de Physique Nucléaire et de Physique des Particules (France), Ministry of Education and Science, Agency for Atomic Energy and RF President Grants Program (Russia), CAPES, CNPq, FAPERJ, FAPESP and FUNDUNESP (Brazil), Departments of Atomic Energy and Science and Technology (India), Colciencias (Colombia), CONACyT (Mexico), KRF (Korea), CONICET and UBACyT (Argentina), The Foundation for Fundamental Research on Matter (The Netherlands), PPARC (United Kingdom), Ministry of Education (Czech Republic), Natural Sciences and Engineering Research Council and WestGrid Project (Canada), BMBF (Germany), A.P. Sloan Foundation, Civilian Research and Development Foundation, Research Corporation, Texas Advanced Research Program, and the Alexander von Humboldt Foundation.

[1] B. Allanach *et al.* *"Searching for R-Parity Violation at Run II of the Tevatron"*, hep-ph/9906224 (2000)
"Report of SUGRA working group for RunII of the Tevatron", hep-ph/00003154 (2000)

[2] DØ Collaboration, *"Search for RpV SUSY in the eeℓ (ℓ = e or μ) channel (λ_{121}-coupling)"*, contributed paper to ICHEP 2004, Beijing

[3] `http://www-d0.fnal.gov/detector/`

[4] N.Ghodbane, S.Katsanevas, P.Morawitz, E.Perez, SUSYGEN3, hep-ph/9909499
`http://lyoinfo.in2p3.fr/susygen/susygen3.html`
`http://www-d0.fnal.gov/computing/MonteCarlo/MonteCarlo.html/generators/susygen.html`

[5] A. Djouadi, J.-L. Kneur, G. Moultaka, hep-ph/0211331 (2002), SUSPECT: *"A Fortran Code for the Supersymmetric and Higgs Particle Spectrum in the MSSM"*

[6] T.Söstrand, Leif Lönnblad, PYTHIA 6.2, Physics and Manual, hep-ph/0108264

[7] R. Hamberg, W. L. van Neerven, T. Matsuura *"A complete calculation of the order of α_s^2 corrections to the Drell-Yan K-factor"*, Nuc. Phys. B**359**, 343-405 (1991)

[8] `http://zebu.uoregon.edu/~parton/partonCTEQ.html`

[9] W. Beenakker *et al.* Phys. Rev. Lett. **83**, 3780 (1999)

[10] T. Hebbeker, *"Calculating Upper Limits with Poisson Statistics"*, L3 Note 2633
`http://www.physik.rwth-aachen.de/~hebbeker/l3note-2633.ps`

[11] DØ-collaboration, *"Search for R-parity Violation in Multilepton Final States in $p\bar{p}$ Collisions at sqrt(s)=1.8 TeV"*, Phys. Rev. D Rapid. Comm. **62**, 071701 (2000)

XI. APPENDIX

TABLE IV: All relevant SM-background processes are listed. The quoted cross sections of the Z/γ^* -processes are LO (PYTHIA) only. In the analysis however the cross section is multiplied by the corresponding K-factor [7] depending on the invariant DiMuon-mass on generator-level. The process $W \to \mu\nu$ has been studied and was found to be negligible.

SM-process (M_{Z/γ^*} [GeV])	$\sigma_{MC}\times$BR [pb]	$\mathcal{L}_{MC}$ [pb^{-1}]	N_{gen}
$Z/\gamma^* \to \mu\mu$ (5–15)	3558.0 ± 40.8	61.7	219250
$Z/\gamma^* \to \mu\mu$ (15–60)	336.6 ± 22.1	1309.1	432000
$Z/\gamma^* \to \mu\mu$ (60–130)	181.0 ± 4.2	2541.4	460000
$Z/\gamma^* \to \mu\mu$ (130–250)	1.370 ± 0.022	7299.3	10000
$Z/\gamma^* \to \mu\mu$ (250–500)	0.115 ± 0.002	$161\cdot10^3$	18500
$Z/\gamma^* \to \mu\mu$ (>500)	$(4.60 \pm 0.07)\cdot10^{-3}$	$2065\cdot10^3$	9500
$Z/\gamma^* \to \tau\tau$ (5–15)	3558.0 ± 40.8	84.7	301250
$Z/\gamma^* \to \tau\tau$ (15–60)	336.6 ± 22.1	1280.5	422563
$Z/\gamma^* \to \tau\tau$ (60–130)	181.0 ± 4.2	3618.8	655000
$Z/\gamma^* \to \tau\tau$ (130–250)	1.370 ± 0.022	$833.9\cdot10^3$	114250
$Z/\gamma^* \to \tau\tau$ (250–500)	0.115 ± 0.002	$956.5\cdot10^3$	11000
$Z/\gamma^* \to \tau\tau$ (>500)	$(4.60 \pm 0.07)\cdot10^{-3}$	$2119.6\cdot10^3$	9750
$\Upsilon(1s) \to \mu\mu$	51.8 ± 0.30	632.8	32750
$\Upsilon(2s) \to \mu\mu$	59.4 ± 0.34	542.9	32250
$WW \to \mu\nu + \mu\nu$	0.093 ± 0.002	$223.1\cdot10^3$	20750
$WZ \to e\nu + \mu\mu$	$(8.68 \pm 0.07)\cdot10^{-3}$	$288.0\cdot10^3$	2500
$WZ \to \mu\nu + \mu\mu$	$(8.68 \pm 0.07)\cdot10^{-3}$	$368.6\cdot10^3$	3200
$t\bar{t} \to \mu\mu$ + X	0.068 ± 0.001	$492.6\cdot10^3$	33500

TABLE V: The generated and analyzed signal MC-samples: CC denotes the chargino+chargino and NC the neutralino+chargino production, where C can either be $\tilde{\chi}_1^\pm$ or $\tilde{\chi}_2^\pm$ and N stands for one of the four neutralinos $\tilde{\chi}_{1,2,3,4}^0$. The masses are taken from SUSYGEN whereas the NLO cross sections are obtained with the program GAUGINOS [9].

$\mu < 0$	masses in GeV				cross sections in pb			
point	m_0	$m_{1/2}$	$M_{\tilde{\chi}_1^0}$	$M_{\tilde{\chi}_1^\pm}$	σ_{CC}	σ_{NC}	σ_{tot}	N_{gen}
$\mathcal{P}1neg$	250	140	57.9	109.2	0.435	0.688	1.411	5500
$\mathcal{P}2neg$	250	150	62.0	117.3	0.321	0.498	1.028	5500
$\mathcal{P}3neg$	250	160	66.0	125.4	0.243	0.370	0.764	5500
$\mathcal{P}4neg$	250	180	74.2	141.8	0.173	0.256	0.437	6000
$\mathcal{P}5neg$	250	200	82.4	158.2	0.104	0.149	0.257	5500
$\mathcal{P}6neg$	250	220	90.6	174.8	0.063	0.089	0.155	9000
$\mathcal{P}7neg$	250	240	98.8	191.3	0.040	0.054	0.096	–
$\mu > 0$								
$\mathcal{P}1pos$	250	150	52.4	92.6	0.871	1.537	2.921	9000
$\mathcal{P}2pos$	250	160	57.2	101.4	0.599	1.017	1.962	5500
$\mathcal{P}3pos$	250	170	61.8	110.2	0.467	0.759	1.239	5500
$\mathcal{P}4pos$	250	180	66.3	118.9	0.339	0.538	0.887	5500
$\mathcal{P}5pos$	250	200	75.4	136.5	0.186	0.285	0.477	5500
$\mathcal{P}6pos$	250	220	84.3	154.0	0.107	0.158	0.269	6000
$\mathcal{P}6pos$	250	240	93.0	171.3	0.064	0.091	0.157	9000
$\mathcal{P}7pos$	250	260	101.7	188.6	0.050	0.070	0.098	–

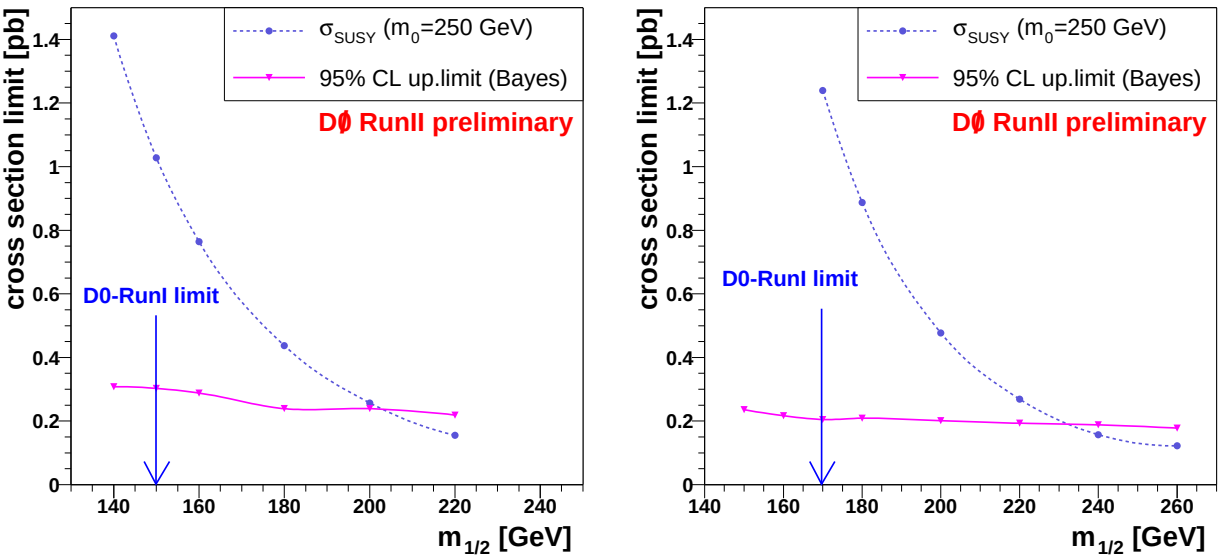

FIG. 6: The 95% CL upper limits on the SUSY cross section (σ_{SUSY}) for fixed m_0 =250 GeV and negative higgsino mass parameter (left) as well as for positive μ (right) is shown.